REPORT DOCUMENTATION PAGE

Form Approved OMB NO. 0704-0188

1. REPORT DATE (DD-MM-YYYY)	2. REPORT TYPE	3. DATES COVERED (From - To)
09-05-2016	Final Report	18-May-2011 - 17-May-2014

4. TITLE AND SUBTITLE
Final Report: Development of Novel Magnetic Metal Oxide Thin Films and Carbon Nanotube Materials for Potential Device Applications

5a. CONTRACT NUMBER
W911NF-11-1-0187

5b. GRANT NUMBER

5c. PROGRAM ELEMENT NUMBER
206022

6. AUTHORS
Keith Jackson, Conrad Williams, Dereje Seifu, Ezana Negresse

5d. PROJECT NUMBER

5e. TASK NUMBER

5f. WORK UNIT NUMBER

7. PERFORMING ORGANIZATION NAMES AND ADDRESSES
Morgan State University
Engineering
1700 East Cold Spring Lane
Baltimore, MD 21251 -0001

8. PERFORMING ORGANIZATION REPORT NUMBER

9. SPONSORING/MONITORING AGENCY NAME(S) AND ADDRESS (ES)
U.S. Army Research Office
P.O. Box 12211
Research Triangle Park, NC 27709-2211

10. SPONSOR/MONITOR'S ACRONYM(S)
ARO

11. SPONSOR/MONITOR'S REPORT NUMBER(S)
58961-MS-REP.3

12. DISTRIBUTION AVAILIBILITY STATEMENT
Approved for Public Release; Distribution Unlimited

13. SUPPLEMENTARY NOTES
The views, opinions and/or findings contained in this report are those of the author(s) and should not contrued as an official Department of the Army position, policy or decision, unless so designated by other documentation.

14. ABSTRACT
Earlier we reported exchange coupling between bilayers of CoFe2O4/CoFe2, where CoFe2O4 and CoFe2 are the hard and soft magnetic layers, respectively. These results suggested that trilayers structures of CoFe2O4/CoFe2/CoFe2O4 are strong candidates for low hysteresis loss “spin spring materials.”To study this possibility, we extended our investigation to the synthesis of CoFe2O4/CoFe2/CoFe2O4 trilayers under different sputtering deposition conditions, which included oxygen pressure in the case of the CoFe2O4 component and the application of a magnetic field during the deposition of the soft CoFe2. The most significant finding was the

15. SUBJECT TERMS
Nanomagnetics, carbon nanotubes, multilayer materials, spin springs, exchange springs, CoFe2O4 films, coercive field, oxygen addition during deposition, applied magnetic field during deposition,uniaxial iron-filled multi-walled carbon nanotubes

16. SECURITY CLASSIFICATION OF:			17. LIMITATION OF ABSTRACT	15. NUMBER OF PAGES	19a. NAME OF RESPONSIBLE PERSON
a. REPORT	b. ABSTRACT	c. THIS PAGE			Keith Jackson
UU	UU	UU	UU		19b. TELEPHONE NUMBER 443-885-3124

Report Title

Final Report: Development of Novel Magnetic Metal Oxide Thin Films and Carbon Nanotube Materials for Potential Device Applications

ABSTRACT

Earlier we reported exchange coupling between bilayers of CoFe2O4/CoFe2, where CoFe2O4 and CoFe2 are the hard and soft magnetic layers, respectively. These results suggested that trilayers structures of CoFe2O4/CoFe2/CoFe2O4 are strong candidates for low hysteresis loss "spin spring materials."To study this possibility, we extended our investigation to the synthesis of CoFe2O4/CoFe2/CoFe2O4 trilayers under different sputtering deposition conditions, which included oxygen pressure in the case of the CoFe2O4 component and the application of a magnetic field during the deposition of the soft CoFe2. The most significant finding was the "blocking field" increased more than 30% by the application of an applied field during deposition of the soft CoFe2, resulting in a decrease in hysteretic losses by a similar percentage. The discussion of spin spring results is in terms of an increase in uniaxial anisotropy energy in the CoFe2 layers due to short range ordering of Fe-Fe and Co-Co pairs during deposition.

We also report on the results of fabrication and measurement of uniaxial iron-filled multi-wall carbon nanotubes. These nanowires required four times higher applied magnetic field (~1500 Oe) to reach saturation compared to planar nanometer thin films of Fe on MgO(100) that reached saturation at around 380 Oe. The results show that Fe nanowires exhibited a two-fold magnetic symmetry.

Enter List of papers submitted or published that acknowledge ARO support from the start of the project to the date of this printing. List the papers, including journal references, in the following categories:

(a) Papers published in peer-reviewed journals (N/A for none)

Received	Paper

TOTAL:

Number of Papers published in peer-reviewed journals:

(b) Papers published in non-peer-reviewed journals (N/A for none)

Received	Paper

TOTAL:

Number of Papers published in non peer-reviewed journals:

(c) Presentations

Vancouver Dr. Williams
Japan Invited Talk Dr. Williams

Number of Presentations: 1.00

Non Peer-Reviewed Conference Proceeding publications (other than abstracts):

Received	Paper

TOTAL:

Number of Non Peer-Reviewed Conference Proceeding publications (other than abstracts):

Peer-Reviewed Conference Proceeding publications (other than abstracts):

Received	Paper	
01/23/2015	2.00	Korey Pough , Abebe Kebede, Dereje Seifu, Destenie Knock . Magnetic Properties of Iron Chalcogenide Superconducting Materials for Energy Storage Applications, March Meeting American Physical Society. 21-MAR-13, . : ,

TOTAL: **1**

Number of Peer-Reviewed Conference Proceeding publications (other than abstracts):

(d) Manuscripts

Received	Paper

TOTAL:

Number of Manuscripts:

Books

Received Book

TOTAL:

Received Book Chapter

TOTAL:

Patents Submitted

Patents Awarded

Awards

Graduate Students

NAME	PERCENT_SUPPORTED
FTE Equivalent:	
Total Number:	

Names of Post Doctorates

NAME	PERCENT_SUPPORTED
Ezana Negresse	1.00
FTE Equivalent:	**1.00**
Total Number:	**1**

Names of Faculty Supported

NAME	PERCENT_SUPPORTED	National Academy Member
Keith Jackson	0.00	
Conrad Williams	0.00	
Dereje Seifu	0.00	
FTE Equivalent:	**0.00**	
Total Number:	**3**	

Names of Under Graduate students supported

NAME	PERCENT_SUPPORTED	Discipline
Jamine Arribas	0.00	Physics
Dominic Smith	0.00	Electrical Engineering
Keion Howard	0.00	Physics
FTE Equivalent:	**0.00**	
Total Number:	**3**	

Student Metrics

This section only applies to graduating undergraduates supported by this agreement in this reporting period

The number of undergraduates funded by this agreement who graduated during this period: 1.00

The number of undergraduates funded by this agreement who graduated during this period with a degree in science, mathematics, engineering, or technology fields:..... 1.00

The number of undergraduates funded by your agreement who graduated during this period and will continue to pursue a graduate or Ph.D. degree in science, mathematics, engineering, or technology fields:..... 1.00

Number of graduating undergraduates who achieved a 3.5 GPA to 4.0 (4.0 max scale):..... 1.00

Number of graduating undergraduates funded by a DoD funded Center of Excellence grant for Education, Research and Engineering:..... 0.00

The number of undergraduates funded by your agreement who graduated during this period and intend to work for the Department of Defense 0.00

The number of undergraduates funded by your agreement who graduated during this period and will receive scholarships or fellowships for further studies in science, mathematics, engineering or technology fields:..... 1.00

Names of Personnel receiving masters degrees

NAME
Total Number:

Names of personnel receiving PHDs

NAME
Not applicable
Total Number: 1

Names of other research staff

NAME	PERCENT_SUPPORTED
FTE Equivalent:	
Total Number:	

Sub Contractors (DD882)

Inventions (DD882)

Scientific Progress

See Attachment

Technology Transfer

FINAL REPORT

Development of Novel Magnetic Metal Oxide Thin Films and Carbon Nanotube Materials for Magnetic Device Applications

Physics Department
Morgan State University
Baltimore, MD 21251

For the period
August 1, 2011 -- July 31, 2014

Supported by
.....
Contract No. W911NF-11-1-0187

Keith H. Jackson, Ph.D.
Principal Investigator

Conrad Williams, Ph.D.
Co-Principal Investigator

Dereje Seifu, Ph.D.
Co-Principal Investigator

Table of Contents

1 Abstract

Earlier we reported exchange coupling between bilayers of $CoFe_2O_4/CoFe_2$, where $CoFe_2O_4$ and $CoFe_2$ are the hard and soft magnetic layers, respectively. These results suggested that trilayers structures of $CoFe_2O_4/CoFe_2/CoFe_2O_4$ are strong candidates for low hysteresis loss "spin spring materials." To study this possibility, we extended our investigation to the synthesis of $CoFe_2O_4/CoFe_2/CoFe_2O_4$ trilayers under different sputtering deposition conditions, which included oxygen pressure in the case of the $CoFe_2O_4$ component and the application of a magnetic field during the deposition of the soft $CoFe_2$. The most significant finding was the "blocking field" increased more than 30% by the application of an applied field during deposition of the soft $CoFe_2$, resulting in a decrease in hysteretic losses by a similar percentage. We will discuss these spin spring results in terms of an increase in uniaxial anisotropy energy in the $CoFe_2$ layers due to short range ordering of Fe-Fe and Co-Co pairs during deposition.

We would also like to report the results of fabrication and unique measurements uniaxial iron-filled multi-wall carbon nanotubes. These measurements include magneto-optic hysteretic properties and torque measurements. These measurements show that the nanowires required four times higher applied magnetic field (~1500 Oe) to reach saturation compared to planar nanometer thin films of Fe on MgO(100) that reached saturation at around 380 Oe. These studies were performed to demonstrate and study the sputter deposition for effective filling of carbon nanotubes. The results show that Fe nanowires, like nanometer Fe films on MgO, exhibited a two-fold magnetic symmetry. Structural and magnetic properties of nanowires and nanometric films studied using XRD showed that a secondary (200) peak of Fe appeared on thin film samples deposited at higher substrate temperatures indicating higher crystalline order but not in the nanowires.

2 *Exchange Spring in ultra-thin $CoFe_2O_4$ /$CoFe_2$ films*

As mentioned in our original proposal, the primary focus of our research is in the areas of thin film and multilayer materials with applications in areas such as magnetic recording, magnetic sensing devices and high frequency planar microwave devices. Emphasis has been placed on programs to investigate the fundamental magnetic and structural properties of non-equilibrium magnetic oxide films and multilayer structures, synthesized by pulsed laser deposition and DC/RF sputter deposition. In pursuing our goals, we investigated the magnetic and structural properties of pulsed laser and sputter deposited multilayer films under different deposition conditions and observed non-equilibrium behaviors. As stated in the original proposal, of particular interest to us, however, were cobalt-ferrite ($CoFe_2O_4$) films and exchange coupled multilayer films of cobalt-ferrite and cobalt iron ($CoFe_2/CoFe_2O_4$) bilayer. Here we present results of our investigations of exchange spring in bilayers and trilayers of $CoFe_2O_4/CoFe_2/CoFe_2O_4$.

Exchange spring magnets (shown in Fig. 2.1 Left) consist of interspersed hard and soft magnetic materials exchanged coupled at the interface [1, 2]. In the past such interspersed materials were the basis for hard magnetic materials/permanent magnets wherein a high magnetic anisotropy hard magnetic material and a high saturation magnetization soft magnetic material were interspersed to obtain a high (BH) energy product permanent magnetic material. Recently, the interest has been in one of the added benefits obtained from these exchanged coupled materials, namely, the large reversible demagnetization, which results in a high permeability. The large reversible demagnetization with little hysteresis loss has been characterized as "exchange spring" hysteresis behavior. The large reversible

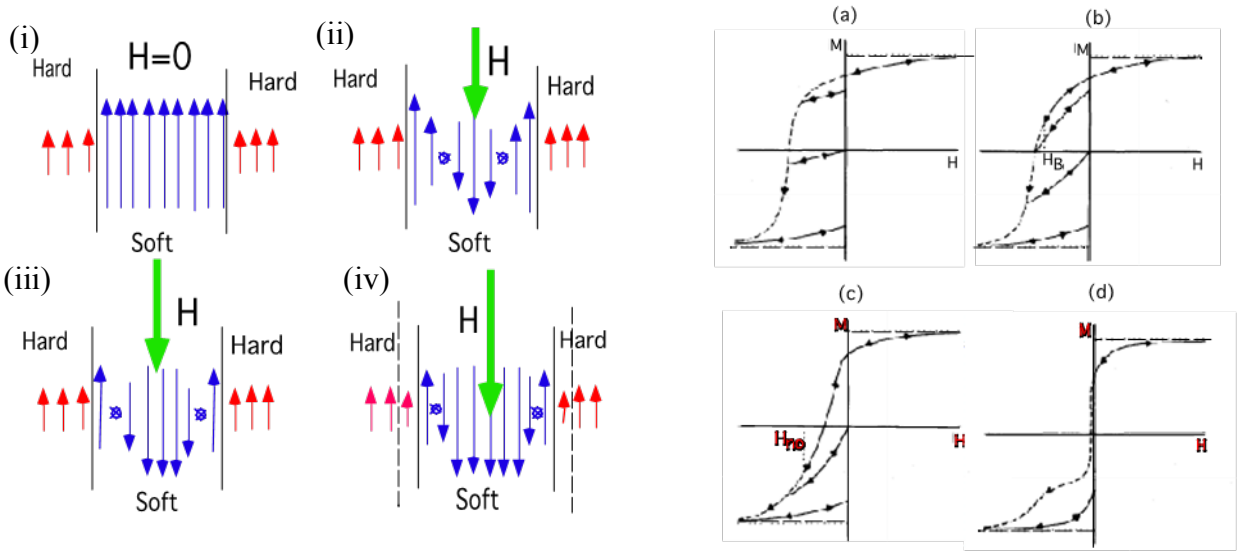

Fig. 2.1 (Left): A schematic diagram showing the spin dynamics of exchange coupling in a trilayer of a soft magnetic layer sandwiched between two hard magnetic layers under the influence of an applied magnetic field (shown by the green arrow) of increasing magnitude from (i) to (iv).

Fig. 2.1 (Right): Loop (a) is the loop expected for magnetic reversal for an ordinary ferromagnetic material, showing hysteresis; loops (b) and (c) are those of an exchange spring material; and loop (d) represents a two phased material, where the magnetic properties of the soft magnetic material dominates between two hard magnetic layers under the application of an applied magnetic field of increasing magnitude.

demagnetization without hysteretic loss has significant technological consequences for many device applications. The essence of this behavior is described in the following: Exchange spring thin film materials are composed of alternating exchanged coupled hard and soft ferromagnetic film layer (Fig. 2.1 Left). As a demagnetizing field is applied, the spins near the center of the soft magnetic layer begin to reverse, while the spins adjacent to the hard magnetic layers remain pinned/unchanged because of exchange coupling between the hard and soft magnetic layer as shown in Fig. 2.1-ii. When the demagnetizing field is reduced to zero the spins "spring" back reversibly to their equilibrium or remnant positions, provided the critical demagnetization field known as the blocking field (H_B) is not exceeded, as in Fig. 2.1-iii. If, the demagnetizing field exceeds the blocking field of the hard magnetic layer, indicated in Fig. 2.1-iv, then the entire spin system switches irreversibly, leading to the more familiar hysteresis and associated energy losses. Schematics of corresponding hysteresis loops are shown in Fig. 2.1 Right. Loop (a) is the expected magnetic reversal for an ordinary ferromagnetic material, showing hysteresis; loops (b) and (c) are those of an exchange spring material; both show magnetic reversal with no hysteresis loss, provided the blocking field is not exceeded; loop (d) represents a two phased material, where the magnetic properties of the soft magnetic materials dominate. The area under the turn-around (recoil) curve represents a larger hysteretic loss.

2.1 Experiment

It is clear that in order to optimize the spin spring behavior in these materials we must first optimize the magnetic properties of the hard ($CoFe_2O_4$) and soft ($CoFe_2$) magnetic materials. Both the hard ($CoFe_2O_4$) and soft ($CoFe_2$) magnetic materials were prepared by RF and DC magnetron sputter deposition, respectively in a well-controlled UHV Sputtering chamber on Silicon wafers. The two basic properties we wished to improve are the coercive force H_c of the hard magnetic film layer and the magnetic anisotropy of the soft magnetic layer. We examined the coercive force of the $CoFe_2O_4$ under various O_2/Ar pressure ratios during magnetron sputtering deposition. We found the introduction of oxygen gas in the chamber during deposition showed a remarkable increase in coercive force H_c; H_c nearly doubled, as shown in Figure 2.2a. Though it is a common practice to add oxygen during the

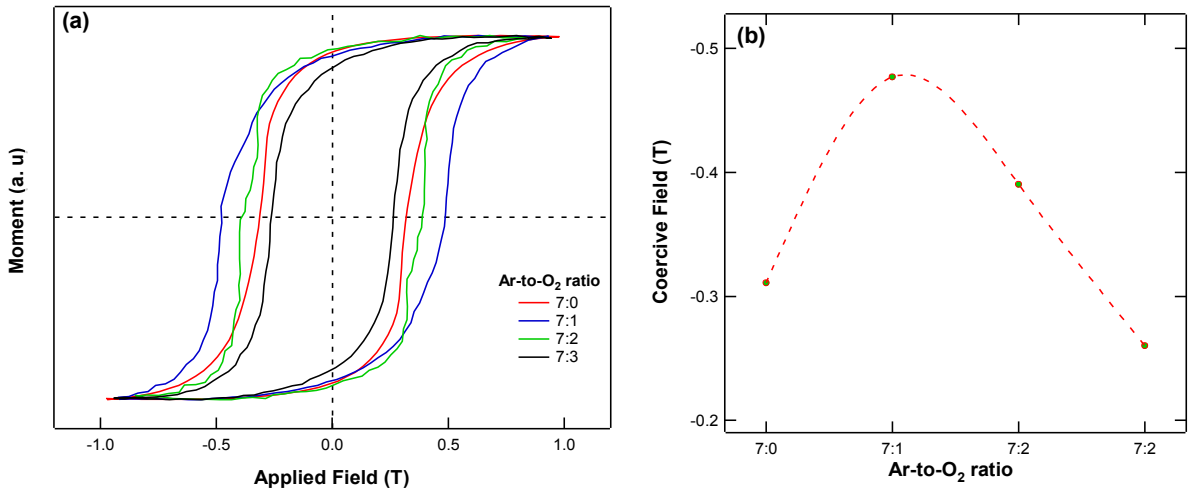

Fig. 2.2: **(a)** Room temperature hysteresis loops at different oxygen concentrations show that adding oxygen improves the coercivity. **(b)** Plotting the effect of adding oxygen on the measured coercive field show the optimal ratio is at 7:1 of argon-to-oxygen

deposition of oxides [3, 4], in the improvement observed in this study is much larger than *any* improvements reported to date by other techniques or processes [5-8]. We found by adding oxygen the coercive field was enhanced from 3.1 to 4.9 kOe. Further, we learned that the addition of oxygen during the deposition was far more consequential than substrate temperature or post-annealing temperature.

Shown in Fig. 2.2 are the room temperature hysteresis loops of samples prepared with argon-to-oxygen ratios of 7:0, 7:1, 7:2 and 7:3. The coercive field peaked at argon-to-oxygen ratio of 7:1. This result shows that over-abundance of oxygen diminishes the coercive field of the hard magnetic layer more than the deficiency of O_2. In a spinel structure the Co^{2+} and Fe^{3+} ions are shared between 16 octahedral and 8 tetrahedral sites while the O_4 atoms are in a close packed cubic arrangement. The magnetic properties depend strongly on the stoichiometry of this structure as indicated by our results and the results of others [4]. Although we have not done X-ray analyses studies or other measurements to accurately determine the stoichiometry of the ferrite, we believe the 7:1 ratio gives the correct stoichiometry.

The next step in this process is to enhance the uniaxial anisotropy of the $CoFe_2$ soft magnetic layer. The idea here is to increase the spin direction uniformity by enhancing the uniaxial anisotropy energy. This will allow a more uniform spin rotation and reversal during magnetization and demagnetization field of the spins in the soft magnetic layer, thereby reducing the hysteretic loss during the spin spring reversal. However, before starting this study we thought it important to study the concept by performing torque and magnetization measurements on two $CoFe_2$ films. One of the films was sputtered in an applied magnetic field of 100 Oe and the other film deposited under the same conditions but in the absence of an applied field. The results of torque and in-plane magnetization measurements as a function of angular rotation in the plane are shown in Fig. 2.3a-b and 2.4, respectively. The $CoFe_2$ sputtered in an applied field clearly shows the development of uniaxial anisotropy energy (see Fig. 2.3) a as evidenced by the development of a *sin 2θ* component in the torque curve, while the film deposited in the absence of a field shows little if any uniaxial anisotropy energy. A similar result is reflected the magnetization measurements

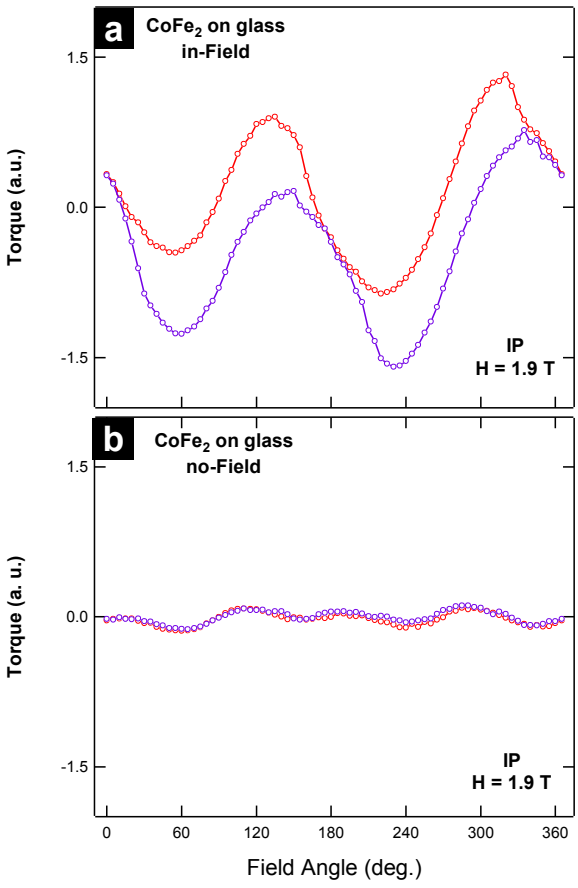

Fig. 2.3: Torque magnetometry for $CoFe_2$ layer deposited (a) in-field and (b) deposited with no-field. Both torque show the in-plane uniaxial anisotropy is induced in the $CoFe_2$ due to the applied field. The torque measurements were done with in-plane field of 1.9 T.

in the film deposited in a magnetic field. These measurements show a distinct easy direction of magnetization in the deposition of the applied magnetic field, as evidenced by the squareness of the hysteresis loop in the 90° direction (Fig. 2.4).

The induced uniaxial anisotropy during deposition in an applied field is directly related to the short-range directional ordering of Fe-Fe pairs in the direction of the applied magnetic field during deposition. Earlier, Schindler and Williams [9] found this to be the case in both bulk and thin film iron-nickel alloys. The ordering of the Fe-Fe pairs requires sufficient atomic mobility at temperatures well below the Curie temperature so as not to destroy the possibility of dipole-dipole interactions between Fe-Fe pairs and Co-Co pairs. However, in the work of Williams and Schindler [10, 11] pair ordering was obtained in thin films by He^3 irradiation in an applied magnetic field at temperatures well below the Curie temperature. In our case, however the atoms are sufficiently mobile during deposition to have an opportunity to develop these pairs upon arrival on the substrate. We plan to extend these studies in the future to exploit these finding in other magnetic systems.

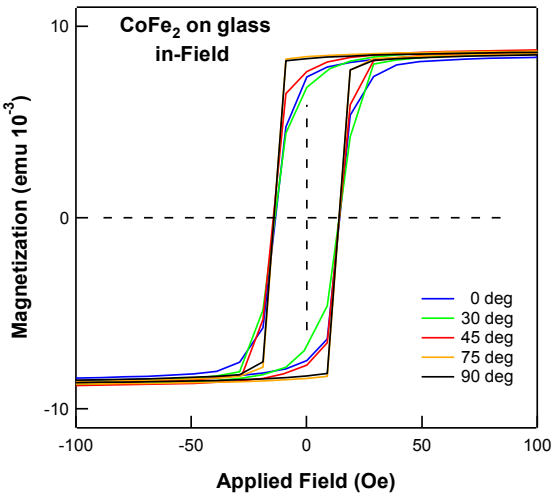

Fig. 2.4: Angle-dependent hysteresis loops for $CoFe_2$ layer deposited in-field show the in-plane uniaxial anisotropy is induced in the $CoFe_2$ due to the applied field. No angle dependence is observed in hysteresis loops for the $CoFe_2$ layer deposited with no applied field.

2.2 Results and Discussion

As indicated earlier, the characteristics that describe the qualities of an exchange spring are the H_B (blocking field), the field at which the hard layer begins to switch and the hysteretic energy loss represented by A_{Rec} the normalized area under the demagnetization curve upon field reversal. For an ideal exchange spring, it is desirable to have H_B equal to or greater than the coercive field, H_c if possible. If the field is reversed prior to reaching H_B no or little hysteresis loss is observed. However, if H_B is exceeded, the loop opens and hysteresis is observed, representing an energy loss (green curve in Fig. 2.5).

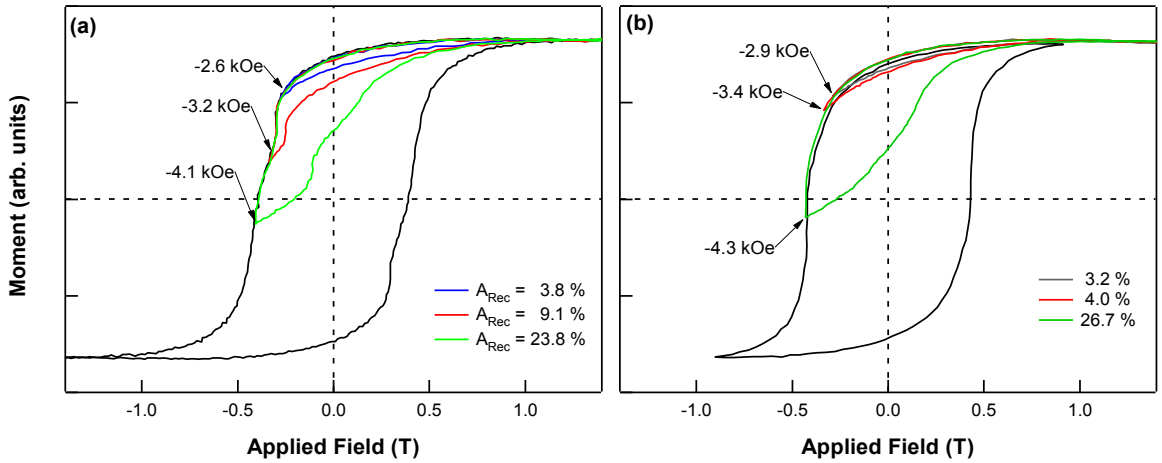

Fig. 2.5: Out-of-plane *recoil* and full hysteresis measurements to for $CoFe_2O_4/CoFe_2/CoFe_2O_4$ trilayer deposited with no-field **(a)** and trilayer deposited in-field **(b)**. The blocking field (H_B), the field where the energy loss is about 5%, for the no-field and in-field trilayers is -2.6 kOe and -3.4 kOe respectively. Depositing the trilayer in-field resulted in a 30% improvement in the blocking field.

Fig. 2.5 shows the results of magnetization measurements for $CoFe_2O_4/CoFe_2/CoFe_2O_4$ trilayers deposited with and without an applied magnetic field during the deposition of the $CoFe_2$ layer. The exchange spring measurement for the trilayer whose soft layer was deposited without an applied field is shown on the left (Fig. 2.5-a) and layer deposited with an applied field is on the right (Fig. 2.5-b). The most significant findings were the "blocking field" increased more than 30% by the application of an applied field during deposition of the soft $CoFe_2$ layers and a similar percentage decrease is shown in the hysteretic loss, as reflected by a comparison of the areas under the curves in Figs. 2.5, respectively.

2.3 Summary

We report exchange spring in sputter deposited trilayers of $CoFe_2O_4/CoFe_2/CoFe_2O_4$. Depositing the ferromagnetic hard layer $CoFe_2O_4$ in the presence of oxygen enhanced coercive field. We found the ratio of 7:1 of argon-to-oxygen yielded the highest coercive field of about 4.9 kOe by balancing the stoichiometry of the cobalt-ferrite. We also enhanced the blocking field of the trilayer by depositing the soft magnetic layer in an applied field. Compared to a sample prepared with no applied field, applying a field during deposition resulted in a 30% enhancement. Our results show that applying magnetic field during deposition induces magnetic anisotropy due to the increased pair ordering in the soft magnetic layer that enhances the uniform rotation of the soft magnetic layer during demagnetization, which in turn enhances the spin spring effect.

Impact of funding on the Morgan Research infrastructure

The new instrumentation acquired through this grant and recently received instrumentation acquired through a subsequent AFOSR Grant will allow us to exploit these results by expanding our studies to include multiple trilayer $CoFe_2O_4/CoFe_2/CoFe_2O_4$ systems. To this end we have started the

modification of our UHV pulsed laser deposition system to facilitate the sputtering of $CoFe_2$. Previously, we sputtered the $CoFe_2O_4/CoFe_2/CoFe_2O_4$ trilayers, however because of the inordinate time required to sputter the cobalt ferrite, we decided to use the modified UHV pulsed laser deposition system for the deposition of the multiple trilayer structures. The potential acquisition of Auger and XPS spectroscopy along with existing instrumentation will allow us to explore and characterize the fundamental origins these very interesting results of the above studies as well as other planned studies.

More importantly, however is the impact on students who participated in these studies. Several are pursuing graduate studies in either Materials Science or Physics and others are doing research at Government or related laboratories. Further, the research infrastructure put in place at Morgan State University by the funding from this grant has the potential to impact students well in the future!!

2.4 References

1. E. F. Kneller and R. Hawig, *The exchange-spring magnet: A new material principle for permanent magnets*, IEEE Trans. Magn. **27**, 3588 (1991).
2. E. E. Fullerton, J.S. Jiang, and S.D. Bader, *Hard/soft magnetic hetrostructures: model exchange-spring magnets*, J. Magn. Magn. Mater. **200**, 392 (1999).
3. M. J. Carey, S. Maat, P. M. Rice, R. F. C. Farrow, R. F. Marks, A. Kellock, P. Nguyen and B. A. Gurney, *Spin valves using insulating cobalt ferrite exchange-spring pinning layers*, Appl. Phys. Lett. **81**, 1044 (2002).
4. A. Lisfi, C. M. Williams, L. T. Nguyen, J. C. Lodder, A. Coleman, H. Corcoran, A. Johnson, P. Change, A. Kumar, and W. Morgan, *Reorientation of magnetic anisotropy in epitaxial cobalt ferrite thin films*, Phys. Rev. B **76**, 054405 (2007).
5. J-G Lee, K. PyoChae and J. Chul Sur, *Surface morphology and magnetic properties of $CoFe_2O_4$ thin films grown by a RF magnetron sputtering method*, J. Magn. Magn. Mater.**267**, 161 (2003)
6. J-P Zhou, H-C He, and C-W Nan, *Effects of substrate temperature and oxygen pressure on the magnetic properties and structures of $CoFe_2O_4$ thin films prepared by pulsed-laser deposition*, Appl. Surf. Sci. **235**, 7456 (2007).
7. A. Raghunathan, I. C. Nlebedim, D. C. Jiles, and J. E. Snyder, *Growth of crystalline cobalt ferrite thin films at lower temperatures using pulsed-laser deposition technique*, J. Appl. Phys.**107**, 09A516 (2010).
8. X. S. Gao, D. H. Bao, B. Birajdar, T. Habisreuther, R. Mattheis, M. A. Schubert, M. Alexe and D. Hesse, *Switching of magnetic anisotropy in epitaxial $CoFe_2O_4$ thin films induced by $SrRuO_3$ buffer layer*, J. Phys. D: Appl. Phys. **42**, 175006 (2009).
9. A. I. Schindler and C. M. Williams, *Investigations of the Effects of Neutron and He3 Irradiation on the Magnetic Properties of Permalloy Thin Films*, J. Appl. Phys. **35**, 877 (1964).
10. C. M. Williams and A. I. Schindler, *Evidence of Long-Range Order in ^{3}He-Irradiated Permalloy Films*, J. Appl. Phys. 41, 1264 (1970).
11. C. M. Williams and A. I. Schindler, *Composition and irradiation-temperature dependence of the uniaxial anisotropy energy of large-grain iron-nickel alloy thin films*, J. Appl. Phys. 44, 5575 (1973).

3 Fe/MWCNTs/SiO_2 and Nano-films of Fe on MgO

3.1 Introduction

The Seifu group has spent several years gaining research experience in nano-magnetics, synthesizing novel nano-magnetic materials using mechanical alloying [1-4], development of chemical and physical methods to filling nano-tubes [5-8], and studying the proximity effect [9-11]. This research project serves as a base line for future research in the synthesis of multilayered nanowires and nanometer thin films to create tunneling magnetoresistance nanowires/films with high enough magnetoresistance value at room temperature to make it viable for practical applications. The goal is the creation of non-volatile magnetoresistive random access memory (MRAM) and next generation magnetic field sensors [12]. Nanowires of Fe were grown using magnetron sputtering in the interior volume of carbon nanotubes vertically grown on SiO_2 substrate. Nanometer films of Fe on MgO(100) were synthesized at several deposition temperatures also using magnetron sputtering. All samples were capped with Cu at room temperature under vacuum to prevent oxidation. Samples were characterized using x-ray diffraction, scanning electron microscopy (SEM), scanning transmission electron microscopy (STEM), vibrating sample magnetometry (VSM), torque magnetometry (TMM), and magneto-optic Kerr effect (MOKE). The system, Fe/MgO(100), despite its relative simplicity is a collection of systems that reveal unique properties attractive for technological applications, such as giant and tunneling magneto-resistance [13-17] and antiferromagnetic coupling [18, 19], oscillatory coupling [19], and biquadratic exchange coupling [20]. Nanometer films (nanofilms) exhibit an out-of-plane uniaxial surface anisotropy sufficient to overcome a demagnetizing field [13]. This property is crucial for the development of higher density magnetic media. This system is an active research topic in nanomagnetism [21]. MgO is an ideal substrate to grow quasi free standing metal structures to study the effects of reduced dimensionality of metals. The reason being due to the very weak interaction between Fe and MgO predicted theoretically by full-potential linearized augmented-plane-wave-total-energy method [22] and verified experimentally using x-ray photoelectron spectroscopy (XPS) and x-ray absorption spectroscopy (XAS) showing the interface between Fe(001) and MgO(100) to be stable at temperatures up to 670 K [23].

The importance of Fe/MgO system is also demonstrated by the several experimental and theoretical studies on Fe/MgO (100) films [22-27]. Ab-initio calculations yielded optimistic tunneling magnetoresistance ratios (TMR) in excess of 100% [24] for Fe/MgO/Fe. XAS and photoemission experiments observed changes in the 3d band due to evolution of Fe local atoms coordination from a bulk-line situation to a configuration where low dimensionality effects are significant [25]. Salvador *et. al.* [26] showed that for uncapped films of Fe, the magnetocrystalline anisotropy of the films increased with deposition temperature indicating improved crystalline structures. Further it was shown the saturation value of the magnetocrystalline anisotropy (550 Oe corresponding to bulk Fe) was reached at a deposition temperature of 300 °C. Our study on nanometric thin films of Fe/MgO(100) showed maximum saturation magnetization at a deposition temperature of 200 °C. Maximum coercive field occurred at 100 °C, Fig. 3.2(a) would provide experimental evidence for this conclusion, indicative of higher magnetocrystalline anisotropy. The coercive field showed a large decrease at

deposition temperatures of 200 °C and 300 °C. This is correlated with the appearance of Fe(200) peak at $\theta = 65°$ in the XRD for samples deposited at these two high temperatures, Fig. 3.1.

Density functional calculations have shown, application of electric fields has a significant effect on the interface magnetization and magnetocrystalline anisotropy. This is due to change in relative occupancy of 3d-orbitals of Fe atoms on Fe/MgO interface. This suggests possible application of Fe/MgO systems for electrically controlled magnetic data storage, multi-ferroic device [27].

The structural and magnetic properties of nanometer Fe films on MgO(100) and nanowires of Fe prepared in the inside of MWCNTs using magnetron DC-sputtering were studied using XRD, SEM/STEM, VSM, TMM, and MOKE measurements. Magnetic measurements using VSM showed that samples prepared at 100 °C exhibit the highest coercive field ($H_C = 176$ Oe) while samples prepared at 50 °C show high remnant magnetization ($M_R = 119$ emu/g) and samples prepared at 200 °C show the highest saturation magnetization ($M_S = 147$ emu/g), which is 68% of the saturation field of bulk Fe as measured by the force method at room temperature [28].As shown in Fig.3.2(a) the three parameters extracted from a B-H loop H_C, M_R, and M_S are at their maximum values not at one particular rather at different substrate growth temperatures. In our study nanowires of Fe capped with Cu in the interior nanometric volume of MWCNTs vertically grown on SiO_2 exhibited an enhanced magnetic coercivity of 137 Oe. This result is comparable with our recent result of single-walled carbon nanotubes coated with Fe2O3 nanoparticles [11] and exceeds that of graphene coated with Fe_2O_3 nanoparticles [10]. In the past magnetic nanoparticles were filled inside and outside MWCNTs and SWCNTs [5, 8, 29-34] using chemical methods. This work illustrates an alternate method of filling substrate supported MWCNTs to synthesize magnetic nanowires using magnetron sputtering.

3.2 Experiment

Vertically aligned MWCNTs were filled with Fe and capped with Cu in this experiment they were grown using a thermal CVD method [34] on SiO_2 substrates. This method involves exposing silica structures to a mixture of ferrocene and xylene at 770 °C for 10 min. The furnace is pumped down to ~200 mtorr in an argon bleed and then heated to a temperature of 770 °C. The solution of ferrocene dissolved in xylene (~0.01g/ml) is pre-heated in a bubbler to 175 °C and then passed through the tube furnace. The furnace is then cooled down to room temperature. The open ended MWCNTs tips were filled with Fe and capped with Cu using a magnetron sputtering method at a substrate temperature of 100 °C. This substrate temperature yielded in planar samples the highest value of coercive field amongst several other substrate temperatures shown in Fig. 3.2(a).

Nanometer thin films were epitaxially grown on MgO(100) substrates (5mm x 5mm x 50 μm) (from MTI company) using magnetron DC sputtering (AXXIS tool from K. J. Lesker company) at several temperatures. All substrates were degassed at 350 °C in a vacuum of 10^{-7}Torr for 1800 sec and samples were pre and post annealed at a pre-selected deposition temperature for 1800 sec in vacuum. All samples were capped with 5 nm of Cu to prevent oxidation. The source to substrate distance was fixed at 30 cm and the substrate was kept at an angle of 45° while being rotated at a constant rate of 20 rpm for uniformity. Under these conditions epitaxial Fe grow on MgO(100) due to weak interface

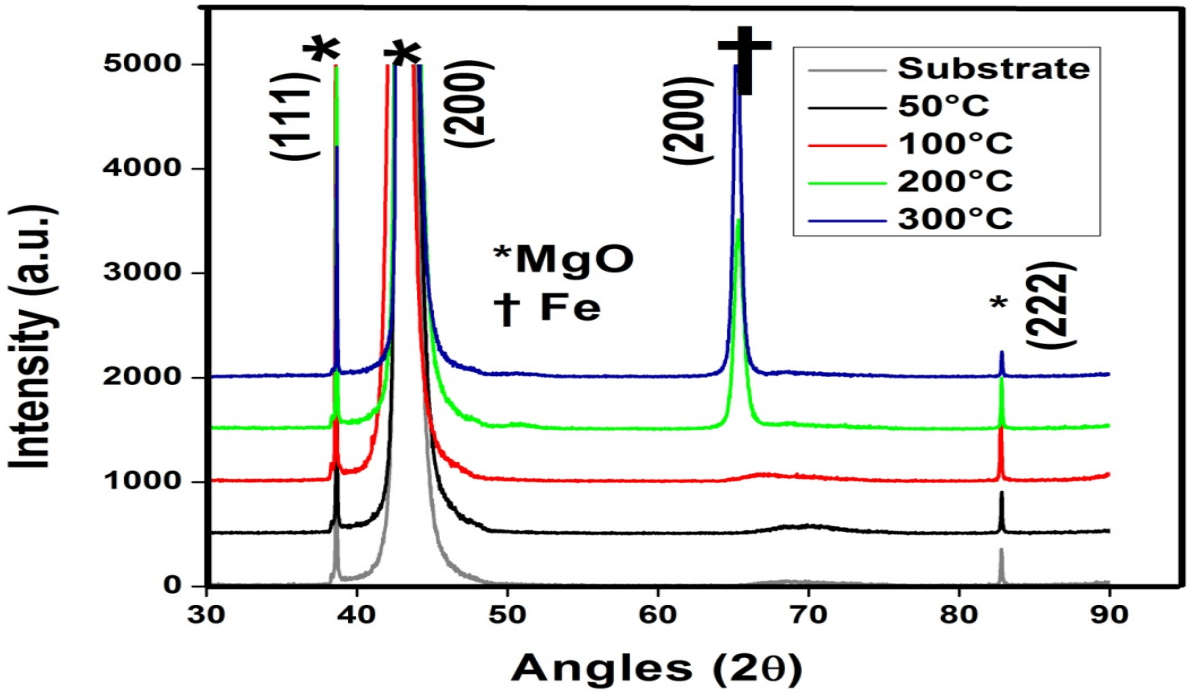

Fig. 3.1: XRD patterns of Fe/MgO(100) deposited at different growth temperatures

interaction [10, 11] a free standing Fe film is formed. The deposition rate for Fe was 0.17nm/s as calibrated by deposition time versus thickness measurements for Fe films several hundred nanometers thick.

Thin film samples of Fe / MgO(100) were characterized by thin film X-ray diffraction (Rigaku D/max Ultima II 40kV/40mA) using CuKα radiation in θ-2θ geometry. Surface morphologies of pristine MWCNTs and nanowires of Fe grown in the nanometric interior volume of MWCNTs were characterized by a Hitachi S-5500 field emission SEM/STEM. For STEM imaging, some nanotubes were scrapped off SiO_2 substrate and dispersed in dimethylformamide the resulting solution was dripped on holey carbon coated carbon TEM grid for SEM and STEM analysis.

VSM measurements were carried out using Vector Magnetometer Model 10 VSM system from MicroSense equipped with 3T electromagnet. Magnetic torque was measured using EV7 TMM system equipped with a 2T electromagnet. MOKE measurements were carried out using an instrument developed at Morgan State University. The basic operating principles of MOKE are based on measuring changes in the polarization of light reflected from a magnetic sample. The MOKE setup consists of a monochromatic light source (HeNe laser, 632 nm wavelength and 5 mW output power), polarizer, analyzer, photodiode, electromagnet, lock-in amplifier, pre-amplifier and an optical modulator. The reflected beam from a magnetic sample is passed through a second polarizer, which serves as the analyzer to select the component of the E-field perpendicular to the plane of incidence. In this geometry the normalized intensity detected is proportional to the component of the magnetization of the sample parallel to the applied magnetic field.

3.3 Results and Discussion

The properties of different crystalline structures are important in magnetism [13]. For this reason one of the goals of this study is to correlate the structure of films with magnetic properties. The structures were characterized by x-ray diffraction using CuKα radiation.

The XRD data displayed in Fig. 3.1are from samples prepared at different temperatures peaked at the same diffraction angle except for samples prepared at substrate temperatures higher than 100 °C.These samples exhibited a (200) sharp peak at an diffraction angle of 65°. This change in crystalline structure and the sharp decrease in coercive field were observed in samples prepared at higher substrate temperatures. This is due to a decrease in magneto-crystalline anisotropy in samples prepared at substrate temperature higher than 100 °C. This result differs from the finding of Salvador et al [26] that magneto-crystalline anisotropy increases monotonously with temperature up to 350 °C.

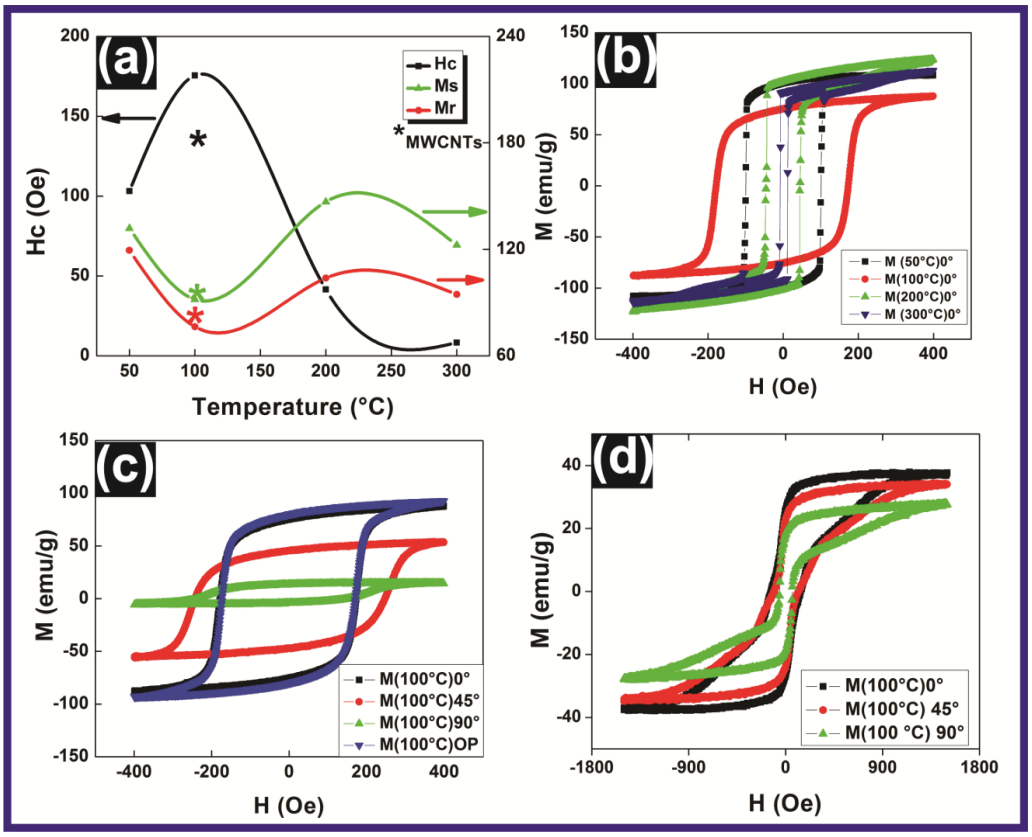

Fig. 3.2: **(a)** Coercive field *vs* growth temperature of Fe/MgO(100) measured with VSM. Coercive field of Fe/MWCNTs nano-wires synthesized at 100 °C indicated by '*'.**(b)** Magnetic hysteresis loops for Fe/MgO(100) films for various growth temperatures as measured by VSM at room temperature. All loops are measured out of plane with the applied field perpendicular to the normal vector to the sample's surface θ=0°.**(c)** Magnetic hysteresis loops for Fe/MgO(100) film prepared at 100 °C at various angles between the normal vector to the surface and the applied magnetic field. The purple loop is for out of plane (OP) measurement θ=0°.**(d)** Magnetic hysteresis loops for Fe/MWCNT wire prepared at 100 °C at various angles between the normal vector to the sample's surface and the applied magnetic field.

Furthermore the XRD data indicates that Fe(200) peak is present at higher deposition temperature this can be understood qualitatively as follows, a Fe atom reaching the substrate at an arbitrary site will not remind for long due to thermal agitation. The higher the temperature the shorter the time the Fe atom will remain at any one site. It will move to a site were the binding energy is high enough that it will not have enough thermal energy to move to another site. XRD of the film deposited at 100 °C does not show a peak at Fe(200), it possesses a maximum coercive field as shown by the VSM data shown in Fig. 3.2(a). A change in crystalline structure and a sharp decrease in coercive field were observed in samples prepared at higher substrate temperatures, the results of VSM room temperature measurements are summarized in Table 3.1.

T (^{o}C)	H_C (Oe)	M_S (emu/g)	M_R (emu/g)	S= M_R/M_S
50	103.0	132.0	119.0	0.906
100	176.0	91.8	76.4	0.832
200	41.6	147.0	104.0	0.707
300	8.3	122.0	94.6	0.773

Table 3.1: VSM measurements of Magnetization values of Fe grown on MgO(100) by magnetron DC sputtering at several deposition temperatures.

Fig. 3.2(a) depicts coercive field (H_C), saturation and remnant magnetization (Ms&Mr) vs. temperature for planar Fe/MgO films as well as nanowire of Fe/MWCNTs. Fig. 3.2(b) VSM measurements of M vs. H for samples synthesized at several substrate temperatures. In Fig.3.2.2(c) and Fig. 3.2(d) M vs. H loops of planar nanometric thin film and nanowire synthesized at a substrate temperature of 100 °C at several angles between the applied field and normal to the surface. The remnant and saturation magnetizations are minima at growth temperature of 100 °C as shown in Fig. 3.2(a). The saturation magnetization, M_S has a maximum value for films deposited at 200 °C for which the coercive field is a minimum. The squareness $S = M_R/M_S$ has a minimum value for films grown at this deposition temperature. This variation is depicted in Fig. 3.2(b) where hysteresis loops for the various Fe/MgO(100) film prepared at several deposition temperatures measured using VSM at room temperature. For the sample with the highest value of H_C, Fig. 3.2(c) depicts, hysteresis loops for various orientation of the magnetic field with the surface normal for Fe/MgO(100) film prepared at 100 °C measured using VSM at room temperature. Listed in Table 3.1 and shown in Fig. 3.2(c) and Fig. 3.2(d) are values of H_C, M_S, and M_R for Fe/MgO(100) planar film and wires of Fe/MWCNTs deposited at 100 °C measured at various angles between the normal vector to the surface and applied magnetic field. H_C was measured to be at its maximum value at 450. M_R and M_S were maximum and H_C at its minimum at 0° and at in-plane orientation. This is another indication that the easy magnetization axis lies in plane and the hard axis out of plane. Seifu *et. al.* [8] showed that the hysteresis loop of Fe-filled MWCNTs exhibits an anomalous narrowing of the loop at the zero magnetization axes. Lopez-Urias, *et. al.* [35] reported formation of helical spin configurations during magnetization of ferromagnetic nanowires encapsulated inside carbon nanotubes.

Maximum coercive field of 176 Oe was observed at synthesis temperature of 100 °C for films and 137 Oe for nanowires, a maximum remnant magnetization of M_R = 120.0 emu/g was observed at 50 °C, a maximum saturation magnetization of M_S = 146.4 emu/g was observed at 200 °C, and the squareness defined S = M_R/M_S was 80% for 2D films and 70% for 1D wire.

Fig. 3.3(a) depicts torque magnetometer measurements at an applied magnetic field of 20 kOe of samples synthesized at several substrate temperatures. In Fig. 3.3(b) MOKE measurements is presented in polar plots. Hysteresis loops were measured using MOKE in longitudinal configuration; from the recoded hysteresis loop the coercive fields of samples were measured as a function of angular position of the sample relative to the applied magnetic field direction, Fig. 3.3(b).

MOKE data indicates the coercive field is a maximum for samples with growth temperature of 100 °C in agreement with VSM. The magnetic torque curve, Fig. 3.3, indicates pronounced 2 fold magnetic symmetry at higher deposition temperature. The torque curve in Fig. 3.3(a) for sample prepared at 100 °C shows less pronounced two-fold symmetry compared to torque curve of samples prepared at higher substrate temperatures. In Fig. 3.3(c) the 100 °C sample shows comparatively higher pronounced at 20 kOe than at lower field strengths there is a transition between 1 kOe and 5 kOe. Fig. 3.3(c) and Fig. 3.3(d) show torque magnetometer measurements of planar film of Fe/MgO(100) and nanowire of Fe/MWCNTs synthesized at 100 °C at several applied fields. Both show similar trend except at low fields the loop for nanowire is off center. Fig. 3.3(b) depicts coercive field measured using MOKE in polar plot for thin films synthesized at several growth temperatures. The same trend is observed in torque magnetometer measurements for lower fields as depicted in Fig. 3.3(c).

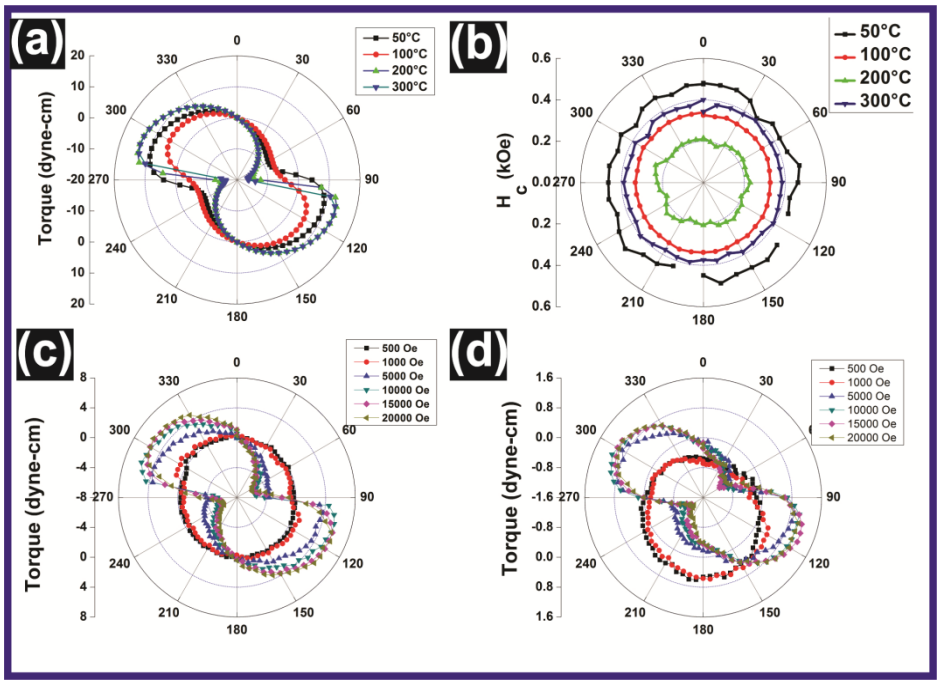

Fig. 3.3: **(a)** Magnetic torque curves of Fe/MgO(100) films for different growth temperatures measured at room temperature in an applied field of 20kOe. **(b)** Magneto-optical longitudinal Kerr loops of Fe/MgO(100) films for various growth temperatures measured at room temperature. **(c)** Magnetic torque curves of Fe/MgO(100) films at growth temperature of 100 °C measured at different applied field strengths at room temperature. **(d)** Magnetic torque curves of Fe/MWCNTs wires at growth temperature of 100 °C measured at different applied field strengths at room temperature.

3.4 Conclusion

In conclusion we have synthesized Cu capped Fe/MgO(100) nanometric thin films and Cu capped nanowires of Fe using MWCNTs as templates. Nanowires were grown at an optimized condition set by growing planar films at several deposition temperatures that showed the best magnetocrystalline property. Magnetic measurements showed that nanowires exhibited higher anisotropy requiring higher saturation field compared to planar thin films due to magnetic shape anisotropy however, similar magnetic symmetry, two-fold, was observed in nanometric films and nanowires. The squareness of nanowires is 10% less than that of planar nanometric thin films.

3.5 References

[1] D. Seifu, F.W. Oliver, E. Hoffman, A. Aning, V.S. Babu, M.S. Seehra, R.M. Catchings, Study of mechanical alloying of Sm and Fe, Journal of applied physics, 81 (1997) 5805-5807.

[2] D. Seifu, F.W. Oliver, E. Hoffman, A. Aning, V.S. Babu, M.S. Seehra, Magnetic properties of nanoscale Sm0.25Zr0.75Fe3 produced by mechanical alloying, Journal of Magnetism and Magnetic Materials, 189 (1998) 305-309.

[3] D. Seifu, A. Kebede, F.W. Oliver, E. Hoffman, E. Hammond, C. Wynter, A. Aning, L. Takacs, I.L. Siu, J.C. Walker, G. Tessema, M.S. Seehra, Evidence of ferrimagnetic ordering in $FeMnO_3$ produced by mechanical alloying, Journal of Magnetism and Magnetic Materials, 212 (2000) 178-182.

[4] D. Seifu, L. Takacs, A. Kebede, ^{151}Eu and ^{57}Fe Mössbauer study of mechanically alloyed $EuFeO_3$, Journal of Magnetism and Magnetic Materials, 302 (2006) 479-483.

[5] D. Seifu, Y. Hijji, G. Hirsch, S.P. Karna, Chemical method of filling carbon nanotubes with magnetic material, Journal of Magnetism and Magnetic Materials, 320 (2008) 312-315.

[6] D. Seifu, S.P. Karna, High Yield Magnetic Nanoparticles Filled Multiwalled Carbon Nanotubes using Pulsed Laser Deposition, in: Nanotechnology, 2008. NANO'08. 8th IEEE Conference on, IEEE, 2008, pp. 778-779.

[7] D. Seifu, S. Karna, Nanomagnetics, in, DTIC Document, 2006.

[8] D. Seifu, G. Mallick, S.P. Karna, Nanomagnetic-Magnetic Nanoparticles Filled Carbon Nanotubes, Nanotechnology Research Journal, 6 (2013) 31.

[9] D. Seifu, S. Neupane, L. Giri, S.P. Karna, H. Hong, M. Seehra, Multilayered graphene acquires ferromagnetism in proximity with magnetite particles, Applied Physics Letters, 106 (2015) 212401.

[10] S. Neupane, H. Hong, L. Giri, S.P. Karna, D. Seifu, Enhanced magnetic properties of graphene coated with Fe2O3 nanoparticles, Journal of Nanoscience and Nanotechnology, 15 (2015) 6690-6694.

[11] S. Neupane, S. Khatiwada, C. Jaye, D.A. Fischer, H. Younes, H. Hong, S.P. Karna, S.G. Hirsch, D. Seifu, Single-walled carbon nanotubes coated by Fe_2O_3 nanoparticles with enhanced magnetic properties, ECS Journal of Solid State Science and Technology, 3 (2014) M39-M44.

[12] S. Wolf, D. Awschalom, R. Buhrman, J. Daughton, S. Von Molnar, M. Roukes, A.Y. Chtchelkanova, D. Treger, Spintronics: a spin-based electronics vision for the future, Science, 294 (2001) 1488-1495.

[13] J.A.C. Bland, B. Heinrich, Ultrathin Magnetic Structures I: An Introduction to the Electronic, Magnetic and Structural Properties, Springer Science & Business Media, 2006.

[14] S. Yuasa, T. Nagahama, A. Fukushima, Y. Suzuki, K. Ando, Giant room-temperature magnetoresistance in single-crystal Fe/MgO/Fe magnetic tunnel junctions, Nat Mater, 3 (2004) 868-871.

[15] D.D. Djayaprawira, K. Tsunekawa, M. Nagai, H. Maehara, S. Yamagata, N. Watanabe, S. Yuasa, Y. Suzuki, K. Ando, 230% room-temperature magnetoresistance in CoFeB/ MgO/ CoFeB magnetic tunnel junctions, Applied Physics Letters, 86 (2005) 092502.

[16] S. Yuasa, A. Fukushima, T. Nagahama, K. Ando, Y. Suzuki, High Tunnel Magnetoresistance at Room Temperature in Fully Epitaxial Fe/MgO/Fe Tunnel Junctions due to Coherent Spin-Polarized Tunneling, Japanese Journal of Applied Physics, 43 (2004) L588-L590.

[17] M. Bowen, V. Cros, F. Petroff, A. Fert, C. MartínezBoubeta, J.L. Costa-Kraïmer, J.V. Anguita, A. Cebollada, F. Briones, J.M. de Teresa, L. Morellón, M.R. Ibarra, F. Güell, F. Peiró, A. Cornet, Large magnetoresistance in Fe/MgO/FeCo(001) epitaxial tunnel junctions on GaAs(001), Applied Physics Letters, 79 (2001) 1655.

[18] P. Grünberg, R. Schreiber, Y. Pang, M. Brodsky, H. Sowers, Layered magnetic structures: evidence for antiferromagnetic coupling of Fe layers across Cr interlayers, Physical Review Letters, 57 (1986) 2442.

[19] S. Parkin, N. More, K. Roche, Oscillations in exchange coupling and magnetoresistance in metallic superlattice structures: Co/Ru, Co/Cr, and Fe/Cr, Physical Review Letters, 64 (1990) 2304.

[20] M. Ruhrig, R. Schafer, A. Hubert, R. Mosler, J. Wolf, S. Demokritov, P. Grünberg, Magnetic properties of ultrathin Fe/Cr/Fe (110) magnetic metallic trilayers “, phys. stat. sol.(a), 125 (1991) 635.

[21] S.D. Bader, Colloquium: Opportunities in nanomagnetism, Reviews of Modern Physics, 78 (2006) 1-15.

[22] C. Li, A. Freeman, Giant monolayer magnetization of Fe on MgO: A nearly ideal two-dimensional magnetic system, Physical Review B, 43 (1991) 780.

[23] P. Luches, S. Benedetti, M. Liberati, F. Boscherini, I.I. Pronin, S. Valeri, Absence of oxide formation at the Fe/MgO(001) interface, Surface Science, 583 (2005) 191-198.

[24] J. Mathon, A. Umerski, Theory of tunneling magnetoresistance in a disorderedFe/MgO/Fe(001)junction, Physical Review B, 74 (2006).

[25] P. Luches, P. Torelli, S. Benedetti, E. Ferramola, R. Gotter, S. Valeri, Structure and electronic properties of Fe nanostructures on MgO (001), Surface Science, 601 (2007) 3902-3906.

[26] C. Salvador, T. Freire, C.G. Bezerra, C. Chesman, E.A. Soares, R. Paniago, E. Silva-Pinto, B.R.A. Neves, Properties of Fe/MgO (1 0 0) nanometric films grown by dc sputtering, Journal of Physics D: Applied Physics, 41 (2008) 205005.

[27] M.K. Niranjan, C.-G. Duan, S.S. Jaswal, E.Y. Tsymbal, Electric field effect on magnetization at the Fe/MgO(001) interface, Applied Physics Letters, 96 (2010) 222504.

[28] J. Crangle, G. Goodman, The magnetization of pure iron and nickel, in: Proceedings of the Royal Society of London A: Mathematical, Physical and Engineering Sciences, The Royal Society, 1971, pp. 477-491.

[29] G. Korneva, H. Ye, Y. Gogotsi, D. Halverson, G. Friedman, J.-C. Bradley, K.G. Kornev, Carbon nanotubes loaded with magnetic particles, Nano letters, 5 (2005) 879-884.

[30] J.-P. Tessonnier, O. Ersen, G. Weinberg, C. Pham-Huu, D.S. Su, R. Schlogl, Selective deposition of metal nanoparticles inside or outside multiwalled carbon nanotubes, Acs Nano, 3 (2009) 2081-2089.

[31] X. Gao, Y. Zhang, X. Chen, G. Pan, J. Yan, F. Wu, H. Yuan, D. Song, Carbon nanotubes filled with metallic nanowires, Carbon, 42 (2004) 47-52.

[32] F. Tan, X. Fan, G. Zhang, F. Zhang, Coating and filling of carbon nanotubes with homogeneous magnetic nanoparticles, Materials letters, 61 (2007) 1805-1808.

[33] D. Jain, R. Wilhelm, An easy way to produce α-iron filled multiwalled carbon nanotubes, Carbon, 45 (2007) 602.

[34] B. Wei, R. Vajtai, Y. Jung, J. Ward, R. Zhang, G. Ramanath, P. Ajayan, Assembly of highly organized carbon nanotube architectures by chemical vapor deposition, Chemistry of materials, 15 (2003) 1598-1606.

[35] F. López-Urías, E. Munoz-Sandoval, M. Reyes-Reyes, A. Romero, M. Terrones, J. Morán-López, Creation of helical vortices during magnetization of aligned carbon nanotubes filled with Fe: Theory and experiment, Physical review letters, 94 (2005) 216102.

4 Impact

The impact of the proposed research on Morgan's overall research environment has been immediate and significant. For our students, most of whom are underrepresented minorities, it provided and still does an opportunity for building analytical and research skills that have applicability across traditional disciplinary boundaries. This also gave our students an opportunity to become involved in the opportunities and technical communities associated with national scientific user facilities. Involvement in the research projects, that this grant will support, gave our students early insights into individual research interests that can be further developed in graduate studies at Morgan State or elsewhere.

4.1 Impact on on-going Research

We introduce undergraduates to our program starting in their freshman year and all things being equal, we keep them through their senior year. In some instances the freshmen that enter our program were a part of our program during their senior year in high school. This has been a very effective method for recruiting students for the Department of Physics.

We use the "Boot Strap Method" method of introducing undergraduate freshman students to research through interactions with peers already in the program. This is a very effective method for creating an undergraduate research culture within the Department of Physics that enhances our program. Our undergraduates spend at least 6-10 hours per week working with the PI or his Post Doc. Since undergraduates do not have much time, considering their course load, either the PI or Post Doc is always available for student training. It should be mentioned that a good Post Doc or Visiting Senior Research Scientist is absolutely necessary to sustain an active research program particularly at a four-year baccalaureate institution where the course load can be challenging.

Each PI had one or two undergraduate students to work directly on their research project. This program supported three undergraduate students and in the 2nd year masters student. The students were from the Physics, Chemistry or Engineering Departments. Students worked closely with the PI's and traveled to light sources to perform experiments. During the summers, students were engaged in research full time at Morgan State University. Although our students are participating in all aspects of the research outlined above, they are assigned specific projects that support the main program. For example, one student is responsible for examining the dependence of hysteretic properties of magnetic oxide thin film surface roughness, as well as the dependence of coercive force H_c on sputter deposition parameters such as laser beam energy, substrate temperature and oxygen pressure.

Equally important is the impact of the requested funding on our faculty. It will help develop and sustain a research program in which they can participate. The funding will also help attract postdoctoral applicants who share our vision of a research-intensive HBCU and may well become candidates for tenure track position as positions become available. Our thin film materials research program has become a catalyst for the attracting faculty with interest in thin film and related condensed matter physics research.

It has attracted several faculty members who in the past have worked in the area of spectroscopy, super conductivity and image spectroscopy. Most of these faculty members conducted their research on bulk magnetic, superconducting and semiconducting materials; now several have shifted their interest to include thin film materials.

4.2 Student Participation

Three students worked at different times and different parts of the project. The students were Jaime Arribas, Dominic Smith and Keion Howard. One of their main tasks was to assist in the synthesis of multilayer exchange spring samples using the sputtering DCA-450 UHV sputtering system and subsequent characterization of the samples. To perform these tasks safely, the students were trained and supervised by the PI's and Post-Docs. To prepare for their work, they were granted access to resources available in the research labs and given hands-on training on all instrumentation and discussions on best practices. All students took part in fabricating and characterizing exchange spring samples. The tasks include (1) cutting, cleaning and mounting substrates for deposition in the DCA-450's load-lock chamber; (2) fabrication of the samples with the designed composition and structure under the specified conditions; (3) characterization of the samples following fabrication using the appropriate equipment available in the lab be it vibrating sample magnetometer, torque magnetometer, scanning electron microscope or thickness measurements using the Profilometer; and (4) analyze the data which in turn lead to further measurements. As they gained experience and understanding of the process, the students actively participated in the design and analysis of the next set of experiments.

In addition to the above stated tasks, the students were given access to resources such as the machine shop and scientific equipment that can be computer-controlled. This was to empower them to explore and discover on their own by working on areas in the project they identified. In the end, each student made a unique contribution to the project in his way. One of the students (Mr. Arribas) has since graduated and is working at the John Hopkins Applied Physics Laboratory. He also paved the way for the other students who followed him by providing guidance and sharing the challenges he had and ways he overcome those challenges.

In broader sense, this introduction and exposure to research had great impact on the students. The approach we took was to get the students involved in the tasks and processes at hand so that they were exposed to the different instrumentation and resources that are available in the lab. At different times the focus of their involvement was such that it provided the students with experience on how research is conducted from designing an experiment to preparing, synthesizing and characterizing the samples followed by interpreting and presenting the results.

In short, as can be inferred from the impact of this experience had on the students, this opportunity demystified working in a research facility and made research accessible. It enabled them to view research as an extension of learning in class and develop deeper appreciation for research while making their unique contributions.

5 Summary

We have already acquired the magnetic characterization instrument, which is already operational. We are waiting for addition equipment in order to complete the work started and furthered by this grant. The impact of this project on the learning experience on students who worked at different phases of the project has been significant. It has also enhanced the research capabilities of Morgan State University and fostered collaborations with in the department and outside the department as well as external collaborators. The on-going research with Dr. Anthony Arrott is a very good example.

We plan to continue this investigation and bring it to fruition for fabricating novel magnetic devices that can be integrated in microchips for applications such as antennae and sensors.

6 List of Figures and Tables